Collective behavior and predation success in a predator-prey model inspired by hunting bats

Yuan Lin and Nicole Abaid*

Department of Engineering Science and Mechanics, Virginia Polytechnic Institute and State University, Blacksburg, Virginia 24061, USA

(Received 26 August 2013; published 30 December 2013)

We establish an agent-based model to study the impact of prey behavior on the hunting success of predators. The predators and prey are modeled as self-propelled particles moving in a three-dimensional domain and subject to specific sensing abilities and behavioral rules inspired by bat hunting. The predators randomly search for prey. The prey either align velocity directions with peers, defined as "interacting" prey, or swarm "independently" of peer presence; both types of prey are subject to additive noise. In a simulation study, we find that interacting prey using low noise have the maximum predation avoidance because they form localized large groups, while they suffer high predation as noise increases due to the formation of broadly dispersed small groups. Independent prey, which are likely to be uniformly distributed in the domain, have higher predation risk under a low noise regime as they traverse larger spatial extents. These effects are enhanced in large prey populations, which exhibit more ordered collective behavior or more uniform spatial distribution as they are interacting or independent, respectively.

DOI: 10.1103/PhysRevE.88.062724 PACS number(s): 87.23.Ge, 05.65.+b, 05.45.Pq, 87.18.Tt

I. INTRODUCTION

Collective behavior is a striking phenomenon observed in animals of diverse species, such as fish swimming in schools [1], birds flying in flocks [2], ants forming organized lanes [3], and mosquitoes flying in swarms [4]. This social behavior is known to provide a variety of benefits for individuals. For example, it may increase the chance for animals to locate food sources [5], conserve heat and energy of a colony [6], help an individual find a mate [7], and reduce the risk of being predated [8]. The benefit of protection from predation, which is of primary interest in this paper, results from the "many eyes" effect [9] and cognitive fusion to predators [10] when animals swarm in groups. The "many eyes" effect enables individuals to have better predator detection through information sharing with peers. An individual's risk of being attacked is diluted by the presence of other group members, which may coalesce into a superorganism in the predator's perception.

Capturing the dynamics of such groups is of interest to a variety of scientific and engineering research questions. In the literature, collective behavior is modeled either through continuum approaches or by establishing agent-based models. For one type of continuum approach, the Navier-Stokes equations are applied to study collective behavior as the motion of a fluid [11,12]; for another continuum-type approach, equations are derived using self-propulsion and velocity reorientation of particles obeying a discrete model [13]. In addition to these modeling efforts, extensive research has been devoted to developing agent-based models, wherein individuals are considered as dynamic particles interacting with peers homogeneously [14]. The agent's behavioral responses are defined using discrete decision making [15,16] or by building potential functions based on the state of the group [17–19]. Among the models defining a decision-making process, common rules applied to individuals for interacting with peers include "repulsion," "alignment," and "attraction." The "repulsion" rule mandates that each individual keeps a certain distance from peers; the "alignment" and "attraction" rules dictate that group members seek consensus in orientations and positions, respectively. Typical models based on such rules and potential functions generate collective behavior [4,20–22] as group-level structures emerge from established principles of behavioral algorithms prescribed to individuals [23].

Research using agent-based models has also tackled the predator-prey relationship; such work finds that the relative population sizes, as well as overall species fitness, can be refined by varying model parameters. In [24], the ranges of sensing for predators and prey are varied to explore a model with carnivorous predators, herbivorous prey, and plants subject to behavioral rules. The authors find that increasing the sensing range for predators is beneficial for individual survival and detrimental for predator population size; analogously, increasing prey sensing range results in a smaller prey population. The steady-state population dynamics of predators and prey are investigated in [25], which finds that agents' initial conditions and the spatial arrangement and availability of resources for prey, such as food and refuge, determine the distribution of system behaviors. We comment that these studies only consider agents moving in discrete two-dimensional domains.

In this paper, we establish an agent-based predator-prey model in a three-dimensional domain to explore the relationship between the collective behavior of prey and predation success. The agents, predators and prey, are modeled as self-propelled particles inspired by rules common to the animal kingdom, that is, both predators and prey sense the environment, and predators hunt for and feed on prey. In the model, the sensing mechanisms and behavioral rules implemented in predators and prey represent the biological system of insectivorous bats and the insects they hunt [26–28]. In particular, predators are equipped with a limited sensing space that is analogous to bats' sonar beam pattern [29,30], which is a key factor in determining their hunting success, and the prey are not capable of sensing the predators. We consider two cases in terms of prey's behavior: (i) prey exhibit collective behavior in the manner of Vicsek [31] by orienting velocity directions with peers subject to additive noise, and

*nabaid@vt.edu

(ii) prey swarm independently as random walkers subject to noise. By comparing simulation results of the two prey-swarming cases, we find that, in a sufficiently large environment, prey forming a few localized cohesive groups have a low chance of being detected by predators. Conversely, if prey are uniformly positioned in the environment, limited rather than extensive traversal of the domain is a better strategy to avoid predation. These results validate the current views held in the biological community that protection from predation is a significant motivator of collective behavior.

II. MODELING

A. Description

We consider a system of $\hat{N}+N$ agents moving in a cube of side length L with periodic boundary conditions in discrete time. In the three-dimensional domain, the agents are partitioned into $\hat{N}$ predators and N prey with constant velocity magnitudes $\hat{s}$ and s, respectively. Each predator has a three-dimensional sensing space, a spherical cone. For the spherical cone, its apex is the predator's position, its side length is the predator's sensing range $\hat{r}_s$, and its opening angle is the predator's angular range of sensing $\hat{\phi}$. The predator's velocity vector starts at the apex of the spherical cone and aligns with its central axis. For predator i, $i=1,2,\ldots,\hat{N}$, the position update at time $t+\Delta t$ is

$$\hat{\mathbf{x}}_i(t+\Delta t)=\hat{\mathbf{x}}_i(t)+\hat{\mathbf{v}}_i(t+\Delta t)\,\Delta t, \tag{1}$$

where t, $\Delta t\in\mathbb{R}^+$, Δt is a constant, and $\hat{\mathbf{x}}_i$, $\hat{\mathbf{v}}_i\in\mathbb{R}^3$ are the predator's position and velocity vectors, respectively.

Each prey has a spherical sensing space whose center is the prey's position and whose radius equals the prey's sensing range r_s. At time t, the position vector of prey k, $k=1,2,\ldots,N$, is $\mathbf{x}_k(t)\in\mathbb{R}^3$ and its velocity vector is $\mathbf{v}_k(t)\in\mathbb{R}^3$. The position update for prey is the same as above for predators in (1). A schematic of the model geometry is shown in Fig. 1.

The initial positions and velocity directions of predators and prey in $\mathbb{R}^3$ are generated with uniformly distributed random probability in the cube of side length L centered at the coordinate origin and in the unit sphere [32], respectively. The state update for both predators and prey depends only on the preceding time step. In the following, we define algorithms to update the velocity directions of predators and prey.

B. Predator velocity update algorithm

In the model, predators are designed to randomly search in the domain until they detect prey, after which they head toward the nearest prey detected. Thus, we define the following two rules to update the velocity directions for predators: a predator heads toward ("hunts") prey if prey are detected, and walks randomly if prey are not detected.

The hunting rule mandates that predators head toward prey that occupy their sensing spaces. When a predator's sensing space is occupied by at least one prey, the predator chooses the nearest prey as a target and orients its velocity direction toward it persistently until the prey is no longer in the sensing space, which is similar to hunting in big brown bats [33]. If the distance between the predator and the prey is less than the eating range $\hat{r}_e$ in the sensing space, the prey is considered to be "eaten." In this case, the prey's position and velocity vectors are randomly reassigned with uniform distribution at the next time step, which results in a prey population of fixed size. When the hunted prey is eaten, the predator chooses the next closest prey in its sensing space and keeps on hunting. We comment that prey that are isolated are not preferentially selected as targets of predators, since the periodic boundary conditions constrain the prey population by design. We define the set of prey that occupy predator i's sensing space at time t as $\mathcal{N}_i(t)$ and the index of the prey targeted as k^*. Then the hunting velocity update for the predator is

$$\hat{\mathbf{v}}_i^h(t+\Delta t)=\hat{s}\,\frac{\mathbf{x}_{k^*}(t)-\hat{\mathbf{x}}_i(t)}{\|\mathbf{x}_{k^*}(t)-\hat{\mathbf{x}}_i(t)\|},\quad k^*\in\mathcal{N}_i(t). \tag{2}$$

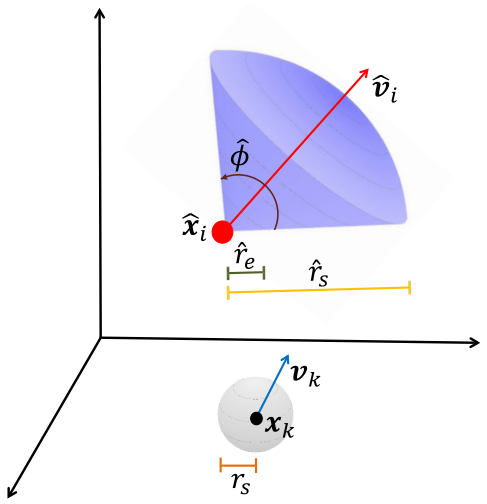

FIG. 1. (Color online) Schematic of three-dimensional sensing geometry for one predator (red circle) and one prey (black circle). The predator i has position $\hat{\mathbf{x}}_i$ and velocity $\hat{\mathbf{v}}_i$; the prey k has position $\mathbf{x}_k$ and velocity $\mathbf{v}_k$. The blue cone shows the predator's sensing space with sensing range $\hat{r}_s$, angular range $\hat{\phi}$, and eating range $\hat{r}_e$. The gray sphere shows the prey's sensing space with sensing range r_s.

If there are no prey in a predator's sensing space, the predator behaves as an independent random walker. In this case, a predator's velocity direction relies only on its previous velocity perturbed by a random noise defined by a perturbation parameter $\hat{\eta}$. The random-walking velocity update for the predator is

$$\hat{\mathbf{v}}_i^w(t+\Delta t)=\hat{s}\,\frac{\hat{\mathbf{v}}_i(t)+\boldsymbol{\omega}(\hat{\eta})}{\|\hat{\mathbf{v}}_i(t)+\boldsymbol{\omega}(\hat{\eta})\|}, \tag{3}$$

where $\boldsymbol{\omega}(\hat{\eta})\in\mathbb{R}^3$ is a realization of a vector-valued random variable whose magnitude is given by a Gaussian distribution with mean zero and standard deviation $\hat{s}\tan(\hat{\eta}\pi)$ and whose direction is uniformly distributed in the plane that is normal to the predator's velocity direction at time t. The magnitude of $\boldsymbol{\omega}(\hat{\eta})$ is restricted to the interval $[0,\hat{s}\tan(\hat{\eta}\pi)]$, which enforces that the angle between $\hat{\mathbf{v}}_i^w(t+\Delta t)$ and $\hat{\mathbf{v}}_i(t)$ is less than or equal to $\hat{\eta}\pi$. When $\hat{\eta}=0$, the angle between these two vectors is always zero; when $\hat{\eta}=1$, this angle varies between zero and π. Loosely speaking, larger values of $\hat{\eta}$ result in higher random noise added at each time step, and

thus more convoluted trajectories for the predators. To avoid unrealistically large values of this noise, which may occur since the Gaussian distribution is defined in $\mathbb{R}$, the realization of the random variable is regenerated when its magnitude has a value outside the stated interval. This restriction also ensures that the normalization with respect to the random noise term is defined.

We update the predator's velocity using the hunting and random-walking updates as

$$\hat{\mathbf{v}}_i(t+\Delta t) = \begin{cases} \hat{\mathbf{v}}_i^h(t+\Delta t) & \text{for} \quad \mathcal{N}_i(t) \neq \emptyset, \\ \hat{\mathbf{v}}_i^w(t+\Delta t) & \text{otherwise.} \end{cases}$$

We note that predators in the model do not interact with their peers, which is selected to agree with observations on groups of bats that congregate socially but do not move or hunt as a typical collective [34].

C. Prey velocity update algorithm

Based on whether or not prey interact with each other, we define two types of prey behavior to update their velocity directions: interacting prey align velocity directions with peers with Gaussian-distributed random noise, and independent prey swarm randomly in addition to noise.

The alignment ability is defined for interacting prey in three dimensions based on Vicsek's model [35]. If the distance between a prey's position and its peer's position is less than the prey's sensing range r_s, the peer occupies the prey's sensing space. We denote $\mathcal{N}_k(t)$ as the set of indices of prey that occupy prey k's sensing space at time t, with $k \in \mathcal{N}_k(t)$ by convention. Prey k's provisional velocity update, $\mathbf{u}_k(t+\Delta t)$, is given by the average of the velocity vectors of prey $l \in \mathcal{N}_k(t)$. In other words,

$$\mathbf{u}_k(t+\Delta t) = s\,\frac{\sum_{l\in\mathcal{N}_k(t)} \mathbf{v}_l(t)}{\left\|\sum_{l\in\mathcal{N}_k(t)} \mathbf{v}_l(t)\right\|}. \tag{4}$$

The provisional velocity update is perturbed by Gaussian-distributed random noise defined by a perturbation parameter η, which is analogous to random walking for predators defined above. Therefore, we obtain the velocity update for prey k as

$$\mathbf{v}_k(t+\Delta t) = s\,\frac{\mathbf{u}_k(t+\Delta t) + \boldsymbol{\omega}(\eta)}{\|\mathbf{u}_k(t+\Delta t) + \boldsymbol{\omega}(\eta)\|}. \tag{5}$$

Independent prey swarm randomly using a rule analogous to the random walking velocity update in predators [36]. However, independent prey use the noise parameter η similarly to interacting prey. The two types of prey behavior can be achieved by using $r_s \neq 0$ for interacting prey and $r_s = 0$ for independent prey. In other words,

$$\mathbf{u}_k(t+\Delta t) = \mathbf{v}_k(t) \tag{6}$$

for independent prey, since interactions with peers are not considered. With the maximum noise at $\eta = 1$, interactions among prey are totally dominated by noise and both interacting and independent prey exhibit the same random swarming behavior. We note that, although we define interactions among prey based on metric distances in line with [31,35], similar collective behavior also results from prey interacting with peers selected using topological distances [1,2], which may be implemented analogously.

We comment that preys' velocity update is not influenced by predators' behavior because prey do not detect predators in the model. As a result, there is no self-protection in prey from being predated upon. This assumption is in accordance with examples of insectivorous bats' prey, such as flying beetles, which do not evade hunting bats [37]. Moreover, lack of bidirectional perception between predators and prey necessitates the selection of only a single time scale for the decision-making process, which is based on the predators alone since their hunting success is the variable of interest.

III. OBSERVABLES

We define four observables to evaluate the behavior of prey: polarization, cohesion, cell occupancy parameter, and cell coverage. The polarization measures the alignment of prey, the cohesion captures prey grouping, the cell occupancy parameter conveys the spatial distribution of prey grouping, and the cell coverage shows the extent covered by an average prey trajectory. Note that high polarization, cohesion, and cell occupancy parameter values indicate prey collective behavior for moderate or large prey population sizes. Finally, the predation success is quantified as the average number of prey eaten by each predator per time step.

The polarization of prey is calculated as the absolute value of their average normalized velocities [31]. In other words, the prey polarization at time t is

$$p(t) = \frac{1}{N}\left\|\sum_{k=1}^{N} \frac{\mathbf{v}_k(t)}{s}\right\|. \tag{7}$$

The value of $p(t)$ ranges from 0 to 1, where 0 means that prey velocity directions are homogeneously oriented in the unit sphere and 1 means that all prey are moving in the same direction. Note that the polarization is 1 for the number of prey $N = 1$.

We compute the prey cohesion based on the method of average nearest neighbor [38], which allows equally high values when prey form large or small groups. In particular, the cohesion is given by the average distance between prey and their nearest peers [39]. With a reference distance L_d, the prey cohesion at time t is

$$c(t) = \exp\left(-\frac{1}{NL_d}\sum_{k=1}^{N} d_k(t)\right), \tag{8}$$

where

$$d_k(t) = \min_{l\neq k} \|\mathbf{x}_l(t) - \mathbf{x}_k(t)\|, \quad l = 1,2,\ldots,N \tag{9}$$

is the distance between prey k and its nearest peer at time t. The reference distance L_d is defined as the cutoff length between peers that are nominally near and far and thus can be used to tailor the absolute magnitude of cohesion. The cohesion $c(t)$ varies between 0 and 1, where a large value indicates high cohesion.

To obtain the cell occupancy parameter and cell coverage, we divide the cubic domain into cubic cells with equal side length L_c. We select L_c as a factor of L so that the number

of cells is $(L/L_c)^3$, which is an integer. The number of prey in cell m, denoted as $n_o(m,t)$, divided by the total number of prey N is the normalized cell occupancy $o(m,t)$ of the cell at time t. In other words,

$$o(m,t) = \frac{n_o(m,t)}{N}. \tag{10}$$

The normalized cell occupancies of all the cells are sorted by magnitude from greatest to least to obtain the normalized sorted cell occupancy at time t, which quantifies the extent of prey groups similarly to the density profiles considered in [40]. The distribution of the normalized sorted cell occupancy which shows large occupancy values for a small number of cells indicates that prey form a small number of large groups. On the contrary, flatter distributions show that prey individuals are likely to be uniformly distributed in the domain. Since most distributions exhibit approximately exponential decay based on inspection, we average the normalized sorted cell occupancy with respect to time for the simulation and fit it with an exponential probability density function [41], which is

$$f(y,\lambda) = \lambda e^{-\lambda y}, \tag{11}$$

where y is the index of the average sorted cell occupancy for each cell, which is a positive integer between 1 and the total number of cells, f is the average normalized sorted cell occupancy, and λ is the cell occupancy parameter obtained by fitting the above distribution. The value of λ is larger for distributions which are peaked for a small number of cells and exhibit fast decay, and it is smaller for distributions which are approximately constant and exhibit slow decay.

The discrete spatial cells are also used to measure the straightness of prey paths. We define the cell coverage for prey k, denoted as $n_c(k,t)$, to be the number of distinct cells that the prey's trajectory occupies during the time interval $[t,t+\Delta\tau]$ for a constant $\Delta\tau \in \mathbb{R}^+$. Cell coverage with a value of 1 means that the prey resides in the same cell with a convoluted trajectory over the time interval, while a higher cell coverage value means that the prey traverses a large extent of the domain by moving over a fairly straight path. Note that, when computing the cell coverage for prey, we neglect time intervals in which prey are eaten because their positions are regenerated randomly in the domain, which results in discontinuous prey trajectories.

The average number of prey eaten by each predator per time step is obtained to evaluate predation success during simulation. This quantity is calculated as

$$\bar{n}_e = \frac{N_e}{\hat{N}T}, \tag{12}$$

where N_e denotes the total number of prey eaten over the entire simulation length in time steps, defined as T. We comment that this metric is normalized by the number of predators to highlight their ability to hunt in the environment of variable resources and is thus not normalized by the number of prey present.

IV. SIMULATION RESULTS

We seek to determine the parameters of the model for the simulation study by taking inspiration from biological systems. The predators' sensing range is taken as $\hat{r}_s = 5$ m and their angular range of sensing is $\hat{\phi} = 120^\circ$, which are physical parameters from big brown bats, *Eptesicus fuscus* [33,42]. The prey's sensing range is taken as half that of the predators', which is $r_s = 2.5$ m. The predator speed is taken as the bat nominal flying speed 5 m/s [43], and the same proportionality between predator and prey sensing ranges is assumed for their velocities. With the prey velocity smaller than the predators', the predators are likely to achieve predation once they sense prey. We consider the population size of predators as $\hat{N} = 10$ and the side length of the domain as $L = 50$ m, such that the density of predators is 0.08 per 1000 m^3. The low density of predators in the domain ensures sufficiently large space for each predator to hunt and lowers their chance of collisions that are neglected in the model, consistently with collision avoidance in bats' behavior [28]. The perturbation parameter for the predator swarm is $\hat{\eta} = 0.1$, which results in relatively straight trajectories which may occur in bats' flights [44,45].

We take the eating range $\hat{r}_e$ as the distance a predator travels in one time step, which is defined as $\Delta t = 0.1$ s for all simulations. In computing prey cohesion, we take the cutoff length $L_d = 5$ m equal to the diameter of the prey spherical sensing space, which is the threshold above which two prey are not able to interact directly or indirectly through common neighbors. By this definition, two prey separated by L_d have a cohesion of $1/e = 0.368$, which defines a nominally small value for this observable. For the simulation study, we consider the hunting behavior of predators with various prey population sizes ranging from 5 to 1000. Thus, the density of prey varies from 0.04 per 1000 m^3 to 8 per 1000 m^3. The side length of the cubic cells is taken as $L_c = 10$ m, such that the volume of one cell is 1000 m^3 and the total number of cells in the domain is 125. The time interval for prey cell coverage, $\Delta\tau$, is taken as 150 Δt, which gives 37.5 m if a prey travels straight with a velocity of 0.25 m/Δt. This selected time interval ensures that a prey can potentially traverse multiple cells, while eliminating double counting of a periodic trajectory since the maximum distance that a prey travels is less than L. For both cases of interacting prey and independent prey, the prey perturbation parameter η varies from 0 to 1, which enables us to obtain both the minimum and maximum effects from random noise. Table I gives a summary of the parameter values used in the simulation study.

Figure 2 shows exemplary frames of predators and interacting prey swarming in simulations with $N = 500$. We see that, with $\eta = 0$, interacting prey form relatively large groups, while with $\eta = 0.2$, they form small groups comprising a few nearby peers. When $\eta = 1$, interacting prey are likely to be homogeneously positioned in the domain with no observable clusters. Thus, the three representative values of η—0, 0.2, and 1—are considered to be associated with low, moderate, and high noise for prey, respectively. For simulations with independent prey, the distributions of particles in the domain are similar to Fig. 2(c). In addition, the motion of each agent follows a straighter trajectory as the noise is decreased.

TABLE I. Parameter values for predators and prey.

	Predators		Prey		
Parameter	Symbol	Value	Symbol	Value	Unit
Population size	$\hat{N}$	10	N	5, 10, 20, 50, 100, 200, 500, 1000	
Speed	$\hat{s}$	0.5	s	0.25	$\mathrm{m}/\Delta t$
		5		2.5	m/s
Sensing range	$\hat{r}_s$	5	r_s	2.5	m
Perturbation parameter	$\hat{\eta}$	0.1	η	0, 0.02, 0.05, 0.1, 0.15, 0.2, 0.5, 1	
Time interval for cell coverage			$\Delta\tau$	150	Δt
Angular range of sensing	$\hat{\phi}$	120			$^\circ$
Eating range	$\hat{r}_e$	0.5			m
Reference distance for cohesion			L_d	5	m

For the simulation study, we take $T = 25\,000$ time steps as one simulation replicate and average the prey's polarization, cohesion, normalized sorted cell occupancy, cell coverage, and the predator's predation success within each replicate with respect to time. Moreover, the cell occupancy parameter λ for each replicate is obtained by fitting the average normalized sorted cell occupancy to the exponential probability density function; the cell coverage values are obtained for each replicate by partitioning the time series into time intervals of length $\Delta\tau$. Simulations are recorded after excluding an initial transient phase of 10 000 time steps. Fifteen replicates are considered for each set of parameters. The number of replicates and the simulation length are selected to ensure stationarity of the results. In other words, the mean of the averages for the observables over the 15 replicates divided by their standard deviation is less than 10%.

Through observation, we find that the mean polarization, cohesion, and cell occupancy parameter λ values remain practically constant for independent prey of fixed population size as noise is varied; this result is absent for interacting prey. Thus, we report the polarization, cohesion, and cell occupancy parameter values for interacting prey in contour plots as the number of prey N and the prey perturbation parameter η are varied in Figs. 3(a), 3(b), and 3(c), respectively. These quantities are shown for independent prey in plots with varying N only; see the black dashed curves in Figs. 3(d), 3(e), and 3(f). Insets inside these three plots display the contour plots which show vertical striation characteristic of the observables. We comment that many contours do not appear smooth due to the small number of data points for large prey population sizes and the lack of smoothing the raw data.

The polarization, cohesion, and cell occupancy parameter values of independent prey are verified through a Monte Carlo simulation. We comment that the expected value for polarization may be computed analytically as a function of N in terms of random variables defining uniformly distributed points on the unit sphere [32]. However, this procedure requires evaluating $2N$ nested integrals, which poses both analytical and numerical challenges. Due to the nearest-neighbor selection process inherent in the cohesion computation and the sorting of cell occupancies, the cohesion and cell occupancy parameter may not be analytically defined in integral expressions. Thus the Monte Carlo simulation is selected for comparison of these observables to the model simulation. In the Monte Carlo simulation, the particles are assigned with random velocity directions and positions at each time step, thus omitting the dynamics of the model. The Monte Carlo simulations are computed with 10 replicates analogously to the model simulations; observable values are also obtained in the same way as above. The quantities from the Monte

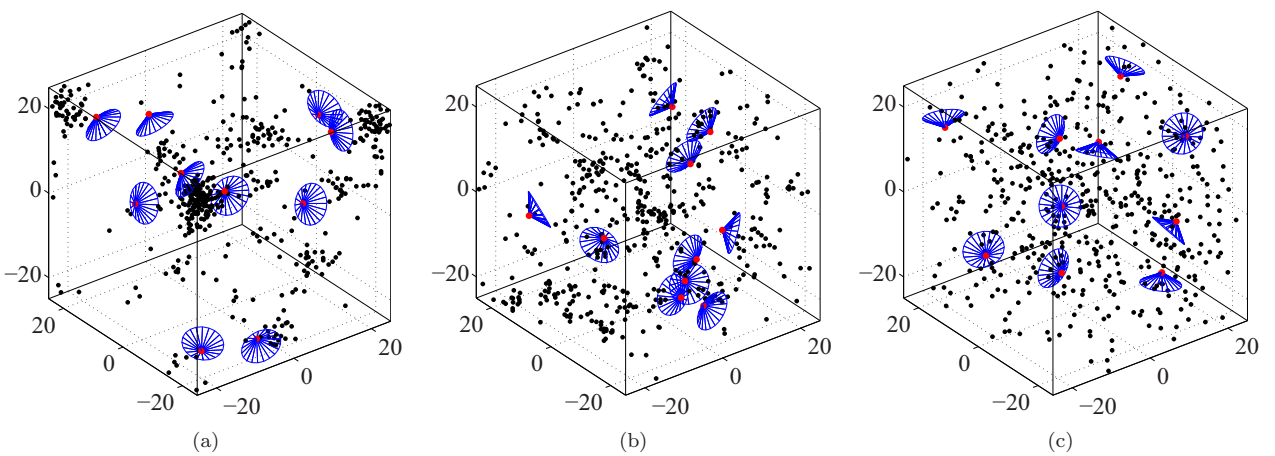

FIG. 2. (Color online) Frames of model simulation with 10 predators and 500 interacting prey when (a) $\eta = 0$, (b) $\eta = 0.2$, and (c) $\eta = 1$. Red dots show predator positions which coincide with the apex of the blue spherical cones showing their sensing spaces; black dots show prey positions. The unit for the numbers on the axes is meters.

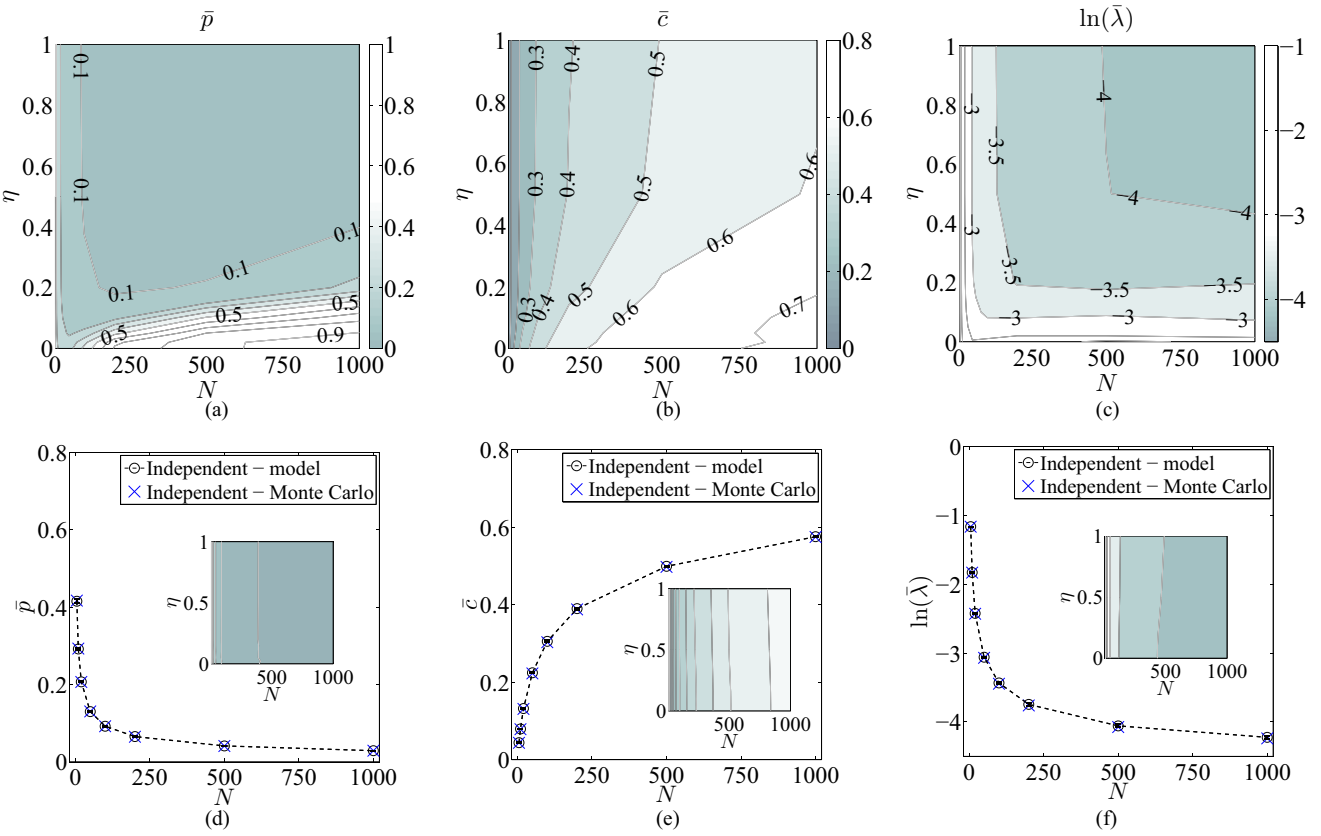

FIG. 3. (Color online) Mean (a) and (d) polarization, (b) and (e) cohesion, and (c) and (f) natural logarithm of the cell occupancy parameter for interacting and independent prey, respectively. Contour plots displayed as prey population size N and perturbation parameter η are varied. The black circles show the mean observable values obtained from the model with independent prey and the blue crosses show results of Monte Carlo simulations. The superscript bar notation denotes the mean over the replicates and the error bars denote standard deviations over all selected values of η. Insets in the second row show contour plots for independent prey. For each inset, the color map is consistent with the contour plot above, that is, with the corresponding observable for interacting prey.

Carlo simulation are denoted as blue crosses in the plots for independent prey.

In Fig. 3(a), we see that the addition of noise is destructive to the polarization of interacting prey. When the noise is low, interacting prey are highly polarized. However, when the noise increases to the moderate level at $\eta = 0.2$, the polarization of interacting prey drops steeply to low values, which are practically constant as the noise increases to its maximum at $\eta = 1$. For a fixed value of noise, there is a nonmonotonic trend accompanied with increasing population sizes for interacting prey: polarization decreases to a minimum value for a relatively small population size and increases as population size grows further. Figure 3(d) shows that the polarization of independent prey decreases with increasing prey population size for all values of noise, as evidenced by the small error bars.

In Fig. 3(b), low noise results in higher cohesion in interacting prey of fixed moderate or large population sizes. This effect is absent in independent prey whose cohesion depends exclusively on N in Fig. 3(e). Generally speaking, cohesion values increase with larger prey population sizes for both interacting and independent prey.

In Fig. 3(c), we see that low noise corresponds to large values of the natural logarithm of the cell occupancy parameter, $\ln(\lambda)$, in interacting prey. Simulations with high noise have low $\ln(\lambda)$ values in interacting prey for moderate or large prey population sizes, similarly to independent prey with all levels of noise in Fig. 3(f). Note that, due to the normalization of the sorted cell occupancy, the fitting gives large $\ln(\lambda)$ values for a small number of prey.

Curves, as opposed to contour plots, are also selected to show the cell coverage for both interacting and independent prey because its values for a fixed prey noise are found to be nearly constant for all prey population sizes N; see the small error bars in Fig. 4. We see that increasing noise results in decreasing cell coverage for both types of prey, which means the prey's trajectories are less straight and cover fewer cells with high prey noise. We comment that the cell coverage for both interacting and independent prey are practically identical, evidencing that random noise rather than the averaging protocol determines the cell coverage values.

The predation success for both interacting and independent prey is shown in contour plots in Fig. 5, as its values vary with both N and η. In Fig. 5(a), we see that interacting prey are least eaten with noise close to zero, while they suffer the highest predation with the moderate noise at $\eta = 0.2$; when noise increases from the moderate value, they have increased protection from predation. Figure 5(b) shows that increasing noise is universally positive to independent prey for avoiding

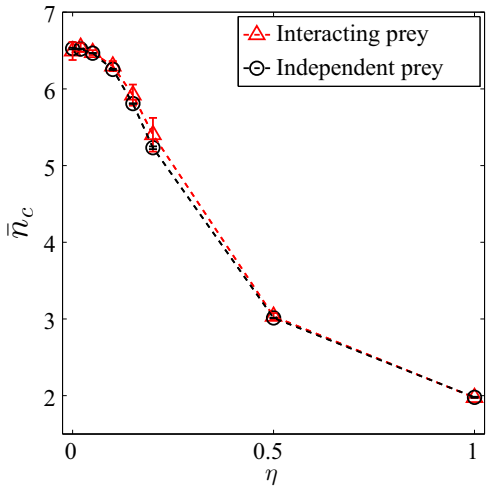

FIG. 4. (Color online) Mean prey cell coverage, as prey perturbation parameter η is varied. The superscript bar notation denotes the mean over the 15 replicates, and the error bars denote standard deviations over all selected values of N.

predation. Moreover, all the above effects about predation success are enhanced with larger prey population sizes.

The relationship between the observables can be observed by computing the correlation coefficient R using a t-test [46]. The test statistic $t = \sqrt{[R^2(\nu-2)/(1-R^2)]}$, where ν is the degrees of freedom. We take $p < 0.05$ as significant. For polarization, cohesion, cell occupancy parameter, and predation success, the correlations are calculated between each pair of observables for all values of N and η considering both the prey population size and noise effects; the quantity ν is the product of the number of perturbation parameter values and the number of prey population sizes tested, which is $8 \times 8 = 64$ in this case. We find that, for interacting prey, the cohesion and cell occupancy parameter are both significantly correlated with predation success (cohesion: $R = 0.89$, $p < 0.01$; cell occupancy parameter: $R = -0.69$, $p < 0.01$) and with each other ($R = -0.67$, $p < 0.01$); on the other hand, the polarization is not correlated with predation success ($R = 0.19$, $p = 0.13$). We further investigate the correlation between cell coverage and predation success for all η values with a fixed N, because cell coverage varies only with noise, as seen in Fig. 4; ν equals 8, the number of perturbation parameter values, in this case. Computing the correlation between cell coverage and predation success for each N of independent prey, we obtain the range of R values $[0.94, 0.97]$ with all $p < 0.01$, which means that cell coverage is significantly correlated to predation success for any prey population size for independent prey.

V. DISCUSSION

Based on the simulation study with varying noise, interaction scheme, and prey population size, we find the following principles regarding predation avoidance: (i) when random noise is sufficiently low, interacting with peers is highly beneficial to avoid predation; (ii) for a prey population of fixed size, there is a maximum probability for interacting

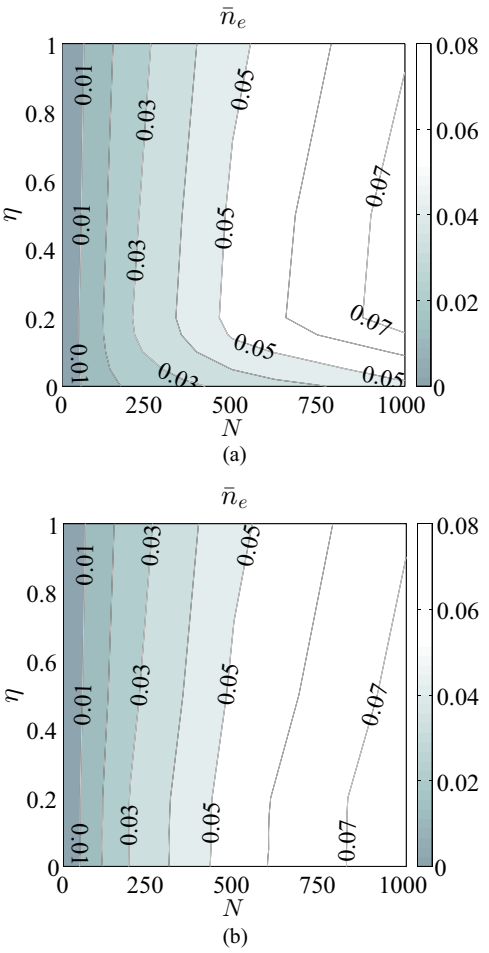

FIG. 5. (Color online) Mean number of eaten (a) interacting and (b) independent prey, as prey population size N and perturbation parameter η are varied.

prey to be eaten when they use noise of a moderate value; and (iii) increasing noise increases the probability to avoid predation for independent prey, an effect that also exists in the case of interacting prey using high noise. Furthermore, these effects are enhanced by increasing the prey population size.

The benefit of protection from predation for interacting prey using low noise results from the formation of large and cohesive groups. For interacting prey, the alignment rule that prey orient velocity directions with peers results in coherent motion of prey, as shown by the high polarization values for $\eta < 0.2$, consistently with [31]. The polarized collective motion induces cohesive prey groups, which confirms the observation in [1] that high polarization corresponds to high cohesion with a similar one-dimensional model. Noise added to the prey's orientation update has a destructive influence on the prey's collective behavior, which is seen by a steep reduction in polarization and cohesion. Further observation through the cell occupancy parameter values for interacting prey shows that lower noise leads to the formation of larger groups. Larger groups result since, with less perturbation to the interaction from noise, prey are more likely to form groups and their coordinated motion is more stable. For sufficiently large

prey population sizes, prey coalescing in a few large groups require the predators to search widely for them, which reduces their probability of being detected and predated. This finding is supported by the negative correlation between cell occupancy parameter values and predation success. Furthermore, this result agrees with the biological literature that cites protection from predation as a primary benefit of collective behavior [47,48]. We comment that, due to its limited sensing space, a predator has low possibility to prey upon sufficiently large prey groups in their entirety, since not all group members are likely to successively occupy its sensing space. This prevents unfettered consumption of large prey populations by predators in the model and thus supports the benefit of forming large groups.

For an interacting prey population of constant size, there is a maximum probability of being predated when the prey form a number of small groups using moderate noise. At the moderate noise level occurring at approximately $\eta = 0.2$, the alignment of interacting prey is perturbed significantly and the prey form small groups compared to the case of low noise, as seen in the cell occupancy parameter values. These small groups occur in relatively large numbers and may move independently in the domain, which corresponds to the sharp decline in polarization. This is supported by the fact that the cohesion reduces less as noise increases, as it is measured in terms of average nearest neighbors. The relatively large number of small groups are likely to be uniformly distributed in the domain, which increases their probability of being detected and predated by predators. In addition, if prey in a small group are detected by a predator, the predator may eat a large portion of the group in contrast to the previously mentioned case of large prey groups. Finally, these trends are supported by the positive correlation between prey cohesion and predation success.

Noise reduces the risk of being detected, and therefore predated upon, when prey swarm independently because high noise results in trajectories with less cell coverage. Independent prey have uniform spatial distribution in the domain, which means that a predator is near prey regardless of its position. When the noise is low, the prey's trajectories are likely to be straight. In contrast, when noise is high, the prey's velocity directions are perturbed at every time step, which results in convoluted trajectories that are likely to cover fewer cells. Since prey are less likely to encounter predators that they are not initially near when their trajectories cover fewer cells, prey using high noise are less likely to be detected and predated upon as a result. The reasoning is supported by the positive correlation between cell coverage and predation success for independent prey. This effect is also evident in interacting prey with noise that is sufficiently high to promote the group's uniform spatial distribution in the domain.

The above effects are all enhanced by larger prey population sizes. For independent prey, the high density of prey in the domain increases the possibility of an individual to encounter predators and get eaten, as prey are likely to be uniformly distributed in the domain. For small interacting prey population sizes, the impact of interacting on the predation success is not obvious since prey's collective behavior fails to emerge for most noise levels. The sensing space of prey occupies only 0.015 71% of the domain volume in the model. Therefore, prey with low density have low chance to interact with peers and do not exhibit emergent collective behavior, as evidenced by the nonmonotonic trend in polarization with minimum values at small prey population sizes. The collective behavior is further hindered as prey are repeatedly eaten and random velocity and position vectors are reassigned for them. This fact can be seen by comparing the polarization values for interacting prey in the presence of predators to the simulations of the Vicsek model in three dimensions in [35], whose values are larger in magnitude. We note that when the number of prey is small, the polarization may be high because a limited number of prey velocity vectors have orientations which are more likely to be inhomogeneously distributed in the unit sphere. This size effect is demonstrated by the nonzero polarization of independent prey computed with both the model and Monte Carlo simulations, which vanishes with increasing group size.

In conclusion, coalescing in localized cohesive groups is an effective strategy for individuals to avoid predation by independent predators. For independent individuals, minimizing the straightness of a path results in decreased predation as opposed to traversing large proportions of the domain, since traveling may expose their positions to predators and increase the risk of being detected. This modeling framework may be translated to diverse applications for studying the dynamics and control of multiagent systems such as animal groups and robotic teams. Similar modeling strategies have been used to model characteristic circular motion in groups of planktonic crustaceans, *Daphnia* [49], and to control teams of robots locating static targets [50].

Future work will include generalizing the model to incorporate more diverse sensing schemes for predators, enabling them to sense and interact with each other [51,52], as is observed in a variety of natural settings [53–55]. Potential emergence in the group of predators will broaden this work to enable exploration of the role of collective behavior in aiding rather than hindering predation. Moreover, prey will be enabled to detect and evade predators [56,57], which is expected to reduce the predation in the simulation and be more relevant to biological systems. The future work is anticipated to find applications in the area of biologically inspired control of robot teams interacting with animal groups [58] or cooperating in dynamic, real-world environments [59,60].

ACKNOWLEDGMENTS

This work is supported by the National Science Foundation under Grant No. EEC-1342176 and by the Institute for Critical Technology and Applied Science at Virginia Tech. The authors would like to thank Dr. M. Porfiri and Dr. M. Aureli for their constructive feedback.

[1] N. Abaid and M. Porfiri, J. R. Soc. Interface **7**, 1441 (2010).

[2] M. Ballerini, N. Cabibbo, R. Candelier, A. Cavagna, E. Cisbani, I. Giardina, V. Lecomte, A. Orlandi, G. Parisi, A. Procaccini,

M. Viale, and V. Zdravkovic, Proc. Natl. Acad. Sci. (USA) **105**, 1232 (2008).
[3] I. D. Couzin and N. R. Franks, Proc. R. Soc. London, Ser. B **270**, 139 (2003).
[4] S. Butail, N. C. Manoukis, M. Diallo, J. M. C. Ribeiro, and D. A. Paley, J. Med. Entomology **50**, 552 (2013).
[5] T. Pitcher, A. Magurran, and I. Winfield, Behav. Ecol. Sociobiol. **10**, 149 (1982).
[6] D. R. Trune and C. N. Slobodchikoff, J. Mammal. **57**, 656 (1976).
[7] D. P. Cowan, J. Animal Ecol. **56**, 779 (1987).
[8] C. C. Ioannou, V. Guttal, and I. D. Couzin, Science **337**, 1212 (2012).
[9] G. Roberts, Animal Behav. **51**, 1077 (1996).
[10] J. Krause and G. D. Ruxton, *Living in Groups* (Oxford University Press, Oxford, UK, 2002).
[11] A. Czirók and T. Vicsek, Physica A **281**, 17 (2000).
[12] J. Toner and Y. Tu, Phys. Rev. E **58**, 4828 (1998).
[13] A. Czirók, A.-L. Barabási, and T. Vicsek, Phys. Rev. Lett. **82**, 209 (1999).
[14] E. Bonabeau, Proc. Natl. Acad. Sci. (USA) **99**, 7280 (2002).
[15] I. Couzin, Nature (London) **445**, 715 (2007).
[16] D. S. Cambu- and A. Rosas, Physica A **391**, 3908 (2012).
[17] M. Aureli and M. Porfiri, Europhys. Lett. **92**, 40004 (2010).
[18] U. Erdmann, W. Ebeling, and A. S. Mikhailov, Phys. Rev. E **71**, 051904 (2005).
[19] J. Strefler, U. Erdmann, and L. Schimansky-Geier, Phys. Rev. E **78**, 031927 (2008).
[20] I. Aoki, Bull. Jpn. Soc. Sci. Fisheries **48**, 1081 (1982).
[21] I. D. Couzin, J. Krause, R. James, G. D. Ruxton, and N. R. Franks, J. Theor. Biol. **218**, 1 (2002).
[22] M. Caratozzolo, S. Carnazza, L. Fortuna, M. Frasca, S. Guglielmino, G. Gurrieri, and G. Marletta, Math. Biosci. Eng. **5**, 75 (2008).
[23] D. J. Sumpter, Philos. Trans. R. Soc. London, Ser. B **361**, 5 (2006).
[24] X. Wang, M. He, and Y. Kang, Physica A **391**, 664 (2012).
[25] M. Droz and A. Pekalski, Phys. Rev. E **63**, 051909 (2001).
[26] J. A. Simmons, M. J. Ferragamo, and C. F. Moss, Proc. Natl. Acad. Sci. (USA) **95**, 12647 (1998).
[27] A. M. Hutson, S. P. Mickleburgh, and P. A. Racey, *Microchiropteran Bats: Global Status Survey and Conservation Action Plan* (IUCN, Gland, Switzerland and Cambridge, UK, 2001).
[28] D. K. Dechmann and K. Safi, Cognition, Brain, Behavior **9**, 479 (2005).
[29] A. Surlykke, S. B. Pedersen, and L. Jakobsen, Proc. R. Soc. London, Ser. B **276**, 853 (2009).
[30] L. Jakobsen and A. Surlykke, Proc. Natl. Acad. Sci. (USA) **107**, 13930 (2010).
[31] T. Vicsek, A. Czirók, E. Ben-Jacob, I. Cohen, and O. Shochet, Phys. Rev. Lett. **75**, 1226 (1995).
[32] G. Grimmett and D. Stirzaker, *Probability and Random Processes* (Oxford University Press, Oxford, UK, 2001).
[33] K. Ghose and C. F. Moss, J. Acoust. Soc. Am. **114**, 1120 (2003).
[34] G. Kerth, M. Wagner, and B. Knig, Behav. Ecol. Sociobiol. **50**, 283 (2001).
[35] H. Chaté, F. Ginelli, G. Grégoire, F. Peruani, and F. Raynaud, Europhys. J. B **64**, 451 (2008).
[36] N. Abaid, E. Bollt, and M. Porfiri, Phys. Rev. E **85**, 041907 (2012).
[37] L. Goldman and O. Henson Jr., Behav. Ecol. Sociobiol. **2**, 411 (1977).
[38] A. Kolpas, J. Moehlis, and I. G. Kevrekidis, Proc. Natl. Acad. Sci. (USA) **104**, 5931 (2007).
[39] M. Aureli, F. Fiorilli, and M. Porfiri, Physica D **241**, 908 (2012).
[40] H. Chaté, F. Ginelli, G. Grégoire, and F. Raynaud, Phys. Rev. E **77**, 046113 (2008).
[41] D. Stirzaker, *Elementary Probability* (Cambridge University Press, Cambridge, UK, 1994).
[42] S. A. Kick, J. Comp. Physiol. A **145**, 431 (1982).
[43] W. W. Au and J. A. Simmons, Phys. Today **60**(9), 40 (2007).
[44] X. Tian, J. Iriarte-Diaz, K. Middleton, R. Galvao, E. Israeli, A. Roemer, A. Sullivan, A. Song, S. Swartz, and K. Breuer, Bioinspiration Biomimetics **1**, S10 (2006).
[45] J. M. V. Rayner and H. D. J. N Aldridge, J. Exp. Biol. **118**, 247 (1985).
[46] R. S. Witte and J. S. Witte, *Statistics* (Wiley, Hoboken, NJ, 2007).
[47] C. P. V. Schaik, Behaviour **87**, 120 (1983).
[48] S. L. Lima and L. M. Dill, Can. J. Zool. **68**, 619 (1990).
[49] A. Ordemann, G. Balazsi, and F. Moss, Physica A **325**, 260 (2003).
[50] K. Sugawara and M. Sano, Physica D **100**, 343 (1997).
[51] R. Cepeda-Gomez, N. Olgac, and D. A. Sierra, IET Contr. Theor. Appl. **5**, 1167 (2011).
[52] D. A. Sierra, P. McCullough, N. Olgac, and E. Adams, Asian J. Contr. **14**, 23 (2012).
[53] D. A. Wiggins, Colonial Waterbirds **14**, 176 (1991).
[54] C. Packer, D. Scheel, and A. E. Pusey, Am. Nat. **136**, 1 (1990).
[55] H. Fritz and M. De Garine-Wichatitsky, J. Animal Ecol. **65**, 736 (1996).
[56] S. L. Lima, Animal Behav. **50**, 1097 (1995).
[57] P. A. Bednekoff and S. L. Lima, Proc. R. Soc. London, Ser. B **265**, 2021 (1998).
[58] G. Polverino and M. Porfiri, Bioinspiration Biomimetics **8**, 044001 (2013).
[59] M. Jadaliha and J. Choi, IEEE Trans. Contr. Syst. Technol. **21**, 899 (2013).
[60] D. Spinello and D. J. Stilwell, in *2011 ASME Dynamic Systems and Control Conference* (ASME, Arlington, VA, 2011), Vol. 1, pp. 25–32.